Weak wave/tide interaction in suspended sediment-stratified flow: a case study

B.A. Kagan[a,b], O. Álvarez[a,c,*], A. Izquierdo[a], R. Mañanes[a], B. Tejedor[a], L. Tejedor[a]

[a]*Departamento de Física Aplicada, Universidad de Cádiz, Apdo. 40, 11510 Puerto Real (Cádiz), Cadiz, Spain*
[b]*Shirshov Institute of Oceanology, Russian Academy of Sciences, St. Petersburg Branch, 30 Pervaya Liniya, 199053 St. Petersburg, Russia*
[c]*Unidad asociada de Oceanografía interdisciplinar Universidad de Cádiz-CSIC. Apdo. 40, 11510 Puerto Real (Cádiz), Spain*

Abstract

The formulation of weak wind-wave/low-frequency current interaction is extended to the case of suspended sediment-stratified flow. The influence of suspended sediment stratification on flow dynamics is described in terms of a sediment stratification parameter defined as von Karman's constant times a depth-independent function of the relative friction velocity and the relative settling velocity of suspended particles that is specified by a solution for the problem on the vertical structure of the suspended sediment-stratified near-bottom logarithmic layer. This 'extended' formulation is inserted in a two-dimensional non-linear, finite-difference, high-resolution hydrodynamic model and the modified model is applied to clarify the roles of wind-wave/tide interaction and suspended sediment stratification—individually and in combination—in the formation of the M_4 and M_6 overtides in Cádiz Bay. It is shown that the predictions for the M_4 and M_6 overtides have much in common and much in contrast with the M_2 tide. For the M_2 tide the influence of suspended sediment stratification shows up most vividly in the spatial variability of the tidal characteristics, but is not evident in changes in the M_4 and M_6 overtides. On the other hand, the influence of wave-induced changes on the M_2 tidal amplitude and phase is only of minor importance, but for the M_4 and M_6 overtides these changes are quite significant. When taken together, the effects of the two factors under investigation are very nearly balanced. This, however, does not mean that the conventional assumption of ignoring these factors is valid in shallow-water dynamics. Simply, that their resulting effect vanishes.
© 2003 Elsevier Science B.V. All rights reserved.

Keywords: wave/tide interaction; suspended sediment stratification; parameterisation; Cádiz Bay

1. Introduction

There are two formulations of wind-wave/low-frequency current interaction. The first (Grant & Madsen, 1979) and its modifications (Christoffersen & Jonsson, 1985; Signell, Beardsley, Graber, & Capotondi, 1990) is based upon the concept of strong wind-wave/low-frequency current interaction. It implies that both wave and low-frequency bottom friction velocity oscillations are enhanced due to their non-linear interaction, so that the bottom friction velocity in a combined (wind-wave + low-frequency current) motion differs from the

sum of the bottom friction velocities induced by pure wave and low-frequency components of motion. The next step in an effort to understand the phenomenon considered was made by Signell et al. (1990) who, following Grant and Madsen (1979), showed that the influence of low-frequency currents on wind waves could be neglected under most conditions. This, in essence, has signalised that the formulation of Grant and Madsen (1979) should be revised.

The second is the weak wind-wave/low-frequency current interaction formulation (Kagan & Utkin, 2000; Kagan et al., 2001). It starts from the evident belief that the interaction between motions with widely different spatial and temporal scales can be weak, even though these motions are in themselves strongly non-linear. This suggests that the bottom friction velocity oscillations with wave and low frequencies are

weakly correlated and, hence, their linear superposition provides an adequate description of the total bottom friction velocity in the combined motion. Clearly, the two formulations differ conceptually from each other.

With regard to particulars, in the first formulation, the vertical eddy viscosity in the wave bottom boundary layer (BBL) is assumed to be dependent on the total bottom friction velocity defined as the square root of the sum of the individual wave and low-frequency components of the bottom stress, but in the second formulation, it is represented as the sum of the two vertical eddy viscosities, each being determined by certain (wave or low frequency) components of the bottom friction velocity in the appropriate BBL in the second one. Furthermore, in the first formulation the vertical eddy viscosity is specified as a linear function of depth, with a slope of von Karman's constant times the total bottom friction velocity in the wave BBL and the current bottom friction velocity above the wave BBL. As a result, the vertical eddy viscosity becomes discontinuous at the top of the wave BBL. In the second formulation the vertical eddy viscosity is taken to be a piecewise linear, continuous function of depth. Another difference lies in the means of obtaining the resistance law for the BBL. For this purpose, Grant and Madsen (1979) and Christoffersen and Jonsson (1985) adopt solutions to the boundary-value problem on the vertical structure of an oscillatory rough turbulent BBL using a priori prescribed vertical eddy viscosity profiles, and Signell et al. (1990) adopting the semiempirical expression of Jonsson (1980) based on laboratory data and the assumption of the logarithmic distribution of velocity throughout the water column. In contrast, Kagan and Utkin (2000) and Kagan et al. (2001) apply the method of matching the asymptotic expansions for velocity in the near-bottom layer and the outer part of the oscillatory rough turbulent BBL, thus avoiding the need to specify any one vertical eddy viscosity profile. Such are the basic distinctions between the formulations.

Strange as it may seem, these apparently dissimilar formulations are satisfactorily consistent with the same field data, in particular the CODE-1 and CODE-2 data (Grant, Williams, & Glenn, 1984) designed specially to verify wind-wave/low-frequency current interaction formulations. In such a situation when the possibilities for experimental verification of either formulation are limited, that formulation is more preferable which is better justified physically and has wider applications. On leaving the choice of a formulation to the discretion of a reader, we now turn our attention to another interesting aspect of the problem.

An evident advantage of the first formulation is that it has been extended to the case of sediment-bearing turbulent flow. This was made by Glenn and Grant (1987) who, following Smith and McLean (1977), described the effect of suspended sediment stratification,

by analogy with the effect of stable thermal stratification in the atmospheric surface layer, in terms of the Monin–Obukhov length scale. A qualitative analogy between the near-bottom logarithmic layer and the atmospheric surface layer does exist. If the change-over of sediment particles into suspension is controlled by the processes of erosion at the sea-bed and entrainment at the top of the bed-load layer, while the vertical distribution of suspended particles is controlled by the processes of turbulent diffusion and gravitational settling, then under non-equilibrium conditions a steady, horizontally homogeneous, sediment-bearing flow can be only stably stratified. In this case, other conditions being the same, the intensity of turbulence will be smaller and the mean velocity will be greater than their values in clear-water flow due to the damping of turbulent kinetic energy by the suspended sediment stratification.

The mere analogy, however, does not mean that the basic conclusions of the Monin–Obukhov similarity theory for the atmospheric surface layer, along with the Monin–Obukhov length scale, can automatically be extended to the suspended sediment-stratified near-bottom logarithmic layer. The reason is the gravitational settling of suspended sediment particles and the associated changes in the vertical direction of the turbulent buoyancy flux and, hence, the Monin–Obukhov length scale. The pronounced changes of the Monin–Obukhov length scale in the suspended sediment-stratified near-bottom logarithmic layer have been widely discussed in the literature. Clearly, the use of the Monin–Obukhov length scale as a parameter of suspended sediment stratification or its associated suspension flux Richardson number can never be wholly effective.

Another way of accounting for the impact of suspended sediment particles on flow dynamics is to employ a sediment stratification parameter, defined as von Karman's constant times a depth-independent function of the relative friction velocity (the ratio of the bottom friction velocity to its critical value at which sediment particles begin to go into suspension) and the relative settling velocity of suspended particles (the ratio of the settling velocity to the bottom friction velocity). In the previous authors' papers (Kagan, Schrimpf, & Utkin, 1999; Álvarez et al., 1999) this parameter was referred to as a 'variable' von Karman's constant. It is specified by a numerical solution to the problem of the vertical structure of the suspended sediment-stratified near-bottom logarithmic layer, followed by the approximation of the vertical velocity profile at different values of the external determining parameters by a logarithmic law.

Here, the weak wind-wave/low-frequency current interaction formulation is extended to sediment-bearing flow by using the sediment stratification parameter to quantify the sediment load effect. In outline, we replace the constant drag coefficient in the conventional parameterisation of bottom friction through the quad-

ratic resistance law by the proper expression following from the 'extended' formulation of weak wind-wave/low-frequency current interaction. Subsequently, this expression is inserted in a two-dimensional (2D) horizontal plane, high-resolution tidal model. On varying the model parameters, comparative analysis is carried out on the roles of wind-wave/tide interaction and suspended sediment stratification in the formation of the M_4 and M_6 overtides in Cádiz Bay which, like other relatively small higher harmonics, are most subjected to these factors. Such are the aims of this paper.

The paper is organised as follows. Section 2 provides the formulation of weak wind-wave/low-frequency current interaction in suspended sediment-stratified flow. Brief information on Cádiz Bay, the investigation site, and the 2D non-linear, finite-difference, high-resolution tidal model incorporating the above formulation is given in Section 3. Section 4 presents the results of the numerical experiments illustrating the role of wind-wave/tide interaction and suspended sediment stratification—individually and in combination—in the dynamics of the M_4 and M_6 overtides in Cádiz Bay. The conclusions are drawn in Section 5.

2. The formulation

As before (see Kagan and Utkin, 2000; Kagan et al., 2001), we assume that: (1) since the characteristic time scale of wind waves is much less than that of any one of tidal constituents, the thickness of the wave BBL is much less than the thickness of the tidal BBL; (2) wind waves are described by linear wave theory, and their influence upon tidal dynamics can be presented in terms of an effective vertical eddy viscosity defined as the sum of the two vertical eddy viscosities each being determined by certain (wind-wave or tidal) components of the motion and considered to be dependent on the bottom friction velocity amplitude in the appropriate BBL; and (3) the effective vertical eddy viscosity is a piecewise, continuous function of the vertical coordinate increasing linearly with distance from bottom within the near-bottom logarithmic layer of wave or tidal origin. In addition, following Kagan et al. (1999) and Álvarez et al. (1999), we now assume that the influence of sediment load on flow dynamics may be accounted for by means of the sediment stratification parameter. Then, on defining the drag coefficient with and without allowance for wind-wave/tide interaction as $c_D^{-1/2} = U_{T1}/U_{*T}$ and $c_{D0}^{-1/2} = \kappa_0^{-1} \ln(z_1/z_0)$, respectively, where U_{*T} is the tidal bottom friction velocity amplitude, z_1 is a reference height within the near-bottom logarithmic layer but above the wave BBL, U_{T1} is the tidal velocity amplitude at this height and κ_0 is von Karman's constant in clear-water flow, the condition of continuity for tidal velocity amplitude at the top of the wave BBL yields,

$$c_D^{-1/2} = \left(\frac{\kappa}{\kappa_0}\right)^{-1} \left\{ c_{D0}^{-1/2} - \frac{1}{\kappa_0}\left[\ln(1+\gamma) + \gamma(1+\gamma)^{-1} \right.\right.$$
$$\left.\left. \ln\frac{\delta_w}{z_0} - \ln\left(1 + \gamma\,\frac{\delta_w}{z_0}\left(\frac{z_1}{z_0}\right)^{-1}\right)\right]\right\}, \tag{1}$$

where

$$\gamma = \frac{U_{*w}}{U_{*T}} \tag{2}$$

is the ratio of the wave bottom friction velocity amplitude, U_{*w}, to U_{*T},

$$\frac{\delta_w}{z_0} = \kappa\,\frac{U_{*w}}{U_{w\infty}}\,Ro_w \tag{3}$$

is the normalised (by the bottom roughness length, z_0) thickness of the wave BBL, $Ro_w = U_{w\infty}/\sigma_w z_0$ is the wave surface Rossby number, $U_{w\infty}$ is the near-bottom wave orbital velocity amplitude, σ_w is wave frequency, κ is the sediment stratification parameter.

The wave and tidal bottom friction velocity amplitudes appearing in Eq. (1) are found from the resistance law for an oscillatory turbulent BBL over a hydrodynamically rough surface. It reads (Kagan et al., 2001)

$$\left[(2.3A)^2 + \left(2.3B + \ln 2^{-5/2}\kappa + \frac{\kappa U_{w\infty}}{U_{*w}}\right)^2\right]^{1/2}$$
$$= \ln Ro_w - \ln\frac{U_{w\infty}}{U_{*w}} + \ln\kappa \tag{4}$$

for the wave BBL and

$$\left[(2.3A)^2 + \left(2.3B + \ln 2^{-5/2}\kappa + \frac{\kappa U_{T\infty}}{U_{*T}}\right)^2\right]^{1/2}$$
$$= \begin{cases} \left(\ln Ro_T - \ln\dfrac{U_{T\infty}}{U_{*T}} + \ln\kappa\right) & \text{if } \delta_T < h, \\[2mm] \ln\dfrac{h}{z_0} & \text{if } \delta_T \geq h \end{cases} \tag{5}$$

for the tidal BBL, in which except for known designations, $Ro_T = U_{T\infty}/\sigma_T z_0$ is the tidal surface Rossby number, $U_{T\infty}$ is the friction-free tidal velocity amplitude, σ_T is the tidal frequency,

$$\frac{\delta_T}{z_0} = \kappa\,\frac{U_{*T}}{U_{T\infty}}\,Ro_T \tag{6}$$

is the normalised (by z_0) tidal BBL thickness, h is the local water depth and A and B are numerical constants equal to 0.92 and 1.38, respectively.

Finally, the sediment stratification parameter, specified following Álvarez et al. (1999), is

$$\kappa = \kappa_0 + 0.0755 \ln\left[\frac{w_s/u_*}{\tan h(0.6(u_*/u_{*c} - 1))}\right]$$
$$- 0.0004(u_*/u_{*c} - 1) \tag{7}$$

if $\kappa \leq \kappa_0$; otherwise, $\kappa = \kappa_0$.

This is solely an heuristic relation, which is obtained by approximating a numerical solution to the equations describing the vertical structure of the suspended sediment-stratified near-bottom logarithmic layer, the range of the external parameters in which this approximation holds good being from 2.0 to 10.0 for u_*/u_{*c} and from 0.1 to 1.0 for w_s/u_*. Here, unlike the definition adopted in Álvarez et al. (1999), $u_* = U_{*T}(1 + \gamma)$ is the total bottom friction velocity amplitude; the remaining designations are the same, namely u_{*c} is the critical bottom friction velocity and w_s is the settling velocity of sediment particles.

Some expressions for c_D in the special cases when the effects of suspended sediment particles or wind waves are disregarded may be found in Álvarez et al. (1999), Kagan and Utkin (2000) and Kagan et al. (2001).

The set of Eqs. (1)–(7) determines uniquely the drag coefficient, c_D, in a wave-affected, suspended sediment-stratified tidal flow, provided that the following five (not three as in the no-suspended sediment case) dimensionless parameters are specified: the ratio of the near-bottom wave orbital velocity amplitude to the friction-free tidal velocity amplitude, $U_{w\infty}/U_{T\infty}$; the wave and tidal surface Rossby numbers, Ro_w and Ro_T; and the normalised (by the friction-free tidal velocity amplitude) critical bottom friction velocity, $u_{*c}/U_{T\infty}$, and settling velocity, $w_s/U_{T\infty}$, of the sediment particles.

A solution to Eqs. (1)–(7) can be readily obtained using an iteration procedure in $U_{*w}/U_{w\infty}$ and $U_{*T}/U_{T\infty}$.

3. The investigation site and the numerical model

The above formulation has been tested in Cádiz Bay where detailed tide-gauge and bottom pressure measurements along the coast and in the interior of the bay have been made during the last few years.

Cádiz Bay is near 36.5°N latitude on the south-west coast of Spain. It faces west toward the Gulf of Cádiz and is landlocked around its south-western, southern and eastern margins by the mainland. The bay is subdivided into two parts, the shallower Inner Bay and the deeper Outer Bay, connected by narrow Puntales Channel (Fig. 1). The bay is relatively shallow, with a maximum depth of 20 m at its seaward edge, and is characterised by predominantly semidiurnal co-oscillating tides with an amplitude of ~1 m for the M_2 constituent. The typical wind waves in Cádiz Bay are short-period waves with periods below 7 s and amplitudes of ~0.5 m in summer and ~1 m in winter. Sea-bed sediments consist mainly of coarse silt with the median grain size of 40 μm and medium sand with the median grain size of 190 μm. Quartz grains comprise 85% of all sediments (Gutiérrez, Achab, & Parrado, 1996).

The 2D vertically integrated, non-linear, finite-difference, high-resolution tidal model developed by Álvarez,
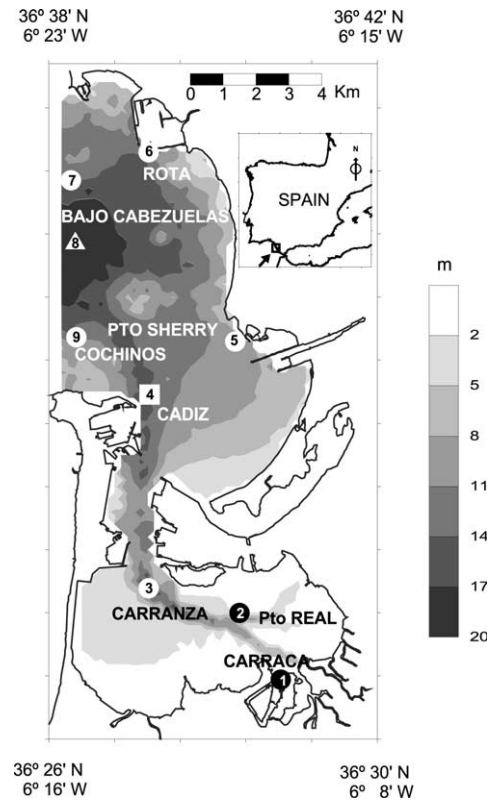
Fig. 1. Map of Cadiz Bay superimposed on the bathymetry (in metres). The location of a tide gauge is denoted by the square; the locations of the bottom pressure sensors, by open and closed circles; and the location of a current meter mooring, by the triangle. A general location map is shown in the inset.

Tejedor and Tejedor (1997) was applied to simulate the fields of tidal elevation and tidal ellipse parameters for the M_4 and M_6 overtides, being defined as higher harmonics generated within a continental shelf in the process of non-linear evolution of the M_2 constituent. A condition of no-flow normal to the coast was set at the land boundaries. At the open boundary, a radiation condition written in terms of deviations of tidal elevation and velocity from their observed values was employed to ensure that, when disturbances were generated, they all propagated away from the model domain. The observed values of tidal elevation along the open boundary were obtained using a linear interpolation/extrapolation of those derived from the bottom pressure measurements at stations Cochinos and Bajo de Cabezuelas, while the observed values of tidal velocity were taken as being equal to the M_2 tidal velocity derived from the data at the current-meter mooring location at the open boundary. Since the simulation of high-precision fields of tidal characteristics is not the prime focus of this paper, the effects of flooding and drying of mud flats have not been considered. Instead, the coastal boundaries are vertical walls at the local water depth of 1 m. The bathymetry was taken out of the IHM chart number 443.

For the solution to be smooth the equations of motion were supplemented by a Laplacian horizontal eddy diffusion operator acting on the tidal velocity throughout the model domain except for its boundaries. The horizontal eddy viscosity was kept, from pure computational considerations, to a minimum of $1 \, \mathrm{m^2 \, s^{-1}}$ to suppress short-wavelength numerical disturbances but, at the same time, to avoid excessively strong smoothing of the derived solution. Additional details of the numerical scheme used may be found in Álvarez et al. (1997, 1999).

The bottom stress related to depth-averaged tidal velocity was parameterised by a quadratic resistance law with the drag coefficient taken as previously described in order to account for the influence of wind-wave/tide interaction and suspended sediment stratification. The reference drag coefficient, von Kármán's constant and the bottom roughness length were set to be $c_{D0} = 0.003$, $\kappa_0 = 0.4$ and $z_0 = 0.1$ cm, respectively. This value of c_{D0} is in approximate agreement with the prescribed value of z_0 and is based upon the reference height 1 m above the bottom. As noted by Heathershaw (1981), z_0 and c_{D0} do not remain constant if there are changes in bed type and bottom sediment grain size. The assumption of constancy of these quantities, however, is likely to be an acceptable approximation for Cádiz Bay where no significant spatial variations in bed types and forms occur. For a detailed discussion of this subject see Aldridge and Davies (1993) and Davies and Lawrence (1995).

Throughout this paper the friction-free tidal velocity amplitude is identified (as is customary for 2D tidal models) with the depth-averaged tidal velocity amplitude. This gives rise to inevitable errors in the bottom stress that depend on local water depth in such a manner that they are larger, the smaller are the depths. The sensitivity of the bottom friction velocity to replacing the tidal velocity at a fixed height above the bottom by the depth-averaged tidal velocity is clarified for the no-wave case in Álvarez et al. (1999).

As an approximate estimate (which falls in the range of the observed values), the mean grain size was prescribed to be 50 μm. Sensitivity results of varying the mean grain size in the no-wave case have been obtained by Álvarez et al. (1999). The settling velocity and the critical bottom friction velocity of sediment particles were determined as functions of mean grain size from the empirical curves depicted by Soulsby and Wainwright (1987).

The near-bottom wave orbital velocity amplitude was calculated from the linear wave theory using known values of wave amplitude, wave frequency and local water depth. Throughout the bay, except for the near-shore shallows, the wave amplitude and frequency were taken to be fixed and equal to their typical summer values of 0.5 m and 7 s. In shallow regions where depths are less than twice the wave amplitude, the latter was assumed to be depth-limited due to wave breaking and equal to the local water depth. This condition is equivalent to the empirical wave breaking criterion employed by Tang and Grimshaw (1996). The applicability of linear wave theory to shallow water was verified by Dean (1986) who, based on a comparison of measured and predicted values of near-bottom wave orbital velocity, showed that this theory provided good results for a wide range of wave amplitude and steepness. The sensitivity of the solution to the problem of interest for the case of clear-water flow to variations in wave parameters was discussed in Kagan et al. (2001).

4. Model results

The modified tidal model was applied in two series of numerical experiments. One of them is intended for performance evaluation of the model; the other, for studies of both factors (wind-wave/tide interaction and suspended sediment stratification) initially isolated and then in combination. Accordingly, the model was first run for the total ($M_2 + M_4 + M_6$) tide assuming that the appropriate values of tidal velocity and elevation appearing in the radiation condition at the open boundary of the bay are known from measurement data. This takes account of the fact that the M_4 and M_6 overtides are generated not only within the bay but also outside it and, hence, are free to be advected from the outer Iberian continental shelf to the bay and back. The neglect of this process causes worse predictions to be obtained than otherwise. This inference is supported by comparison with the observed tidal constants at selected tide-gauge and bottom pressure measurement locations within the bay (see Table 1).

By contrast, when evaluating the influence of the above-mentioned factors upon the M_4 and M_6 tidal dynamics in the bay, the use of any observational data, specifically at the open boundary, is undesirable because these data contain information about the factors under study. In such an event, a standard way is to disregard the observational data at the open boundary, thereby eliminating the contribution of the outer Iberian continental shelf to the formation of overtides in the bay. This technique is applied to perform the following four numerical experiments: a control experiment with none of the factors considered, and three subsequent experiments in which allowances are made sequentially for suspended sediment stratification, wind–wave tide interaction and their combined effect. These numerical experiments are referred to as Experiments 1–4, respectively.

The model predictions results are displayed in Figs. 2–5. The drag coefficient in Experiment 1 is not illustrated because it has a uniform value of 3×10^{-3} throughout the domain. Figs. 2a–5a testify that the M_4 and M_6 overtides (the latter is not shown) are generated in the shallower Inner Bay and Puntales Channel where the non-linear effects responsible for the production of all overtides are

Table 1
Comparison between observed and predicted tidal elevation amplitudes A and phases φ

| N° | Station | Observed | | Predicted | | | | | | | |
| | | | | Experiment 1 | | Experiment 2 | | Experiment 3 | | Experiment 4 | |
		A (cm)	φ (deg)	A (cm)	φ (deg)	A (cm)	φ (deg)	A (cm)	φ (deg)	A (cm)	φ (deg)
M_4 *tidal constituent*											
1	Carraca	2.7	180.0	1.4	356.2	1.3	353.1	3.3	23.2	1.3/1.5	353.3/177.4
2	Pto Real	2.7	167.2	1.3	355.1	1.1	352.2	3.2	22.5	1.2/1.4	352.4/178.1
3	Carranza	2.6	167.1	0.8	18.0	0.8	17.2	1.5	33.1	0.8/1.9	17.2/162.8
4	Cádiz	2.1	154.3	0.5	36.2	0.5	35.5	0.6	47.0	0.5/2.1	35.6/158.8
5	P. Sherry	2.0	157.5	0.5	26.5	0.5	25.6	0.5	37.8	0.5/1.9	25.3/159.9
6	Rota	1.7	160.0	0.3	32.7	0.3	31.5	0.3	43.1	0.3/1.9	31.5/158.3
M_6 *tidal constituent*											
1	Carraca	1.4	85.0	0.5	110.0	0.4	109.5	1.6	118.5	0.4/0.8	109.5/87.5
2	Pto Real	1.1	78.3	0.5	108.5	0.4	108.0	1.6	116.4	0.4/0.8	108.0/89.6
3	Carranza	0.9	83.5	0.4	110.0	0.3	108.0	1.2	128.5	0.3/0.6	109.0/80.8
4	Cádiz	0.2	66.4	0.1	148.5	0.1	138.5	0.1	146.0	0.1/0.2	143.0/65.4
5	P. Sherry	0.2	68.5	0.1	163.0	0.1	158.4	0.1	158.5	0.1/0.2	158.0/67.2
6	Rota	0.3	63.8	0.1	212.2	0.1	210.5	0.1	218.3	0.1/0.1	210.1/62.4

The predicted values of tidal elevation amplitudes and phases, except for those presented to the right of inclined lines, are obtained without allowance for observed tidal characteristics at the open boundary; the remaining predicted values are obtained with allowance.

maximal due to strong spatial changes in the M_2 tidal velocity amplitude and phase. Here, the amplitude of tidal elevation and maximum depth-averaged tidal velocity are predicted to be, respectively, up to 1.5 and 2.5 cm s^{-1} for the M_4 harmonic and 0.5 and 1.5 cm s^{-1} for the M_6 harmonic, being reduced to zero values in Outer Bay as the distance to the open boundary decreases.

As can be seen, the inclusion of the suspended sediment stratification effect (Experiment 2) is followed by a marked decrease in the drag coefficient within Puntales Channel and its vicinities. Here the drag coefficient may be two times smaller than that in clear-water flow (Fig. 2a). This produces a fall in bottom stress and, as a consequence, an increase in maximum depth-averaged tidal velocity (Fig. 3b) and a decrease in tidal elevation amplitude (Fig. 4b) and tidal elevation phase (Fig. 5b). The suspended sediment-induced changes in the M_4 and M_6 maximum depth-averaged tidal velocities are of the same order of magnitude as their typical values in clear-water flow, while the changes in the M_4 and M_6 tidal elevation amplitudes and phases are indeed small. The changes in tidal elevation amplitudes do not exceed 0.1 cm for the M_4 harmonic and 0.2 cm for the M_6 harmonic, which are an order of magnitude smaller than their typical values in Inner Bay. Similarly, the changes in tidal elevation phases do not exceed a few degrees, and are several times smaller than their spatial variations within the domain. This behaviour is in clear contrast to the predictions for the M_2 constituent.

By contrast, in the results of Experiment 3, as might be expected, the drag coefficient in the wave-affected tidal flow increases throughout Cádiz Bay, the most significant changes, up to eightfold over the no-wave case, occurring in Inner Bay. These changes entail a marked enhancement of bottom stress, which is most conspicuous in the regions of strong tidal currents, especially Puntales Channel and the shallows. This, in turn, tends to decrease tidal velocities (Fig. 3c) and to increase tidal elevation amplitudes (Fig. 4c) and phases (Fig. 5c). The decrease in maximum depth-averaged tidal velocity for both the harmonics may be as much as 1.5–3.0 cm s^{-1}, being commensurable with the M_4 and M_6 typical tidal velocities in clear water-flow. Accordingly, the wave-induced changes in the M_4 and M_6 tidal elevation amplitudes and phases may range up to 2.0 cm and 30°, and, as for the M_2 constituent, such changes are mainly detected in Inner Bay. This, however, does not exclude the possibility that, due to the complete dissimilarity between the M_2 tide and the M_4 and M_6 overtides, the role of the wave-induced changes in the formation of the tidal harmonics can be quite different.

In this connection it should be remembered that, according to Davies and Lawrence (1994a,b), the M_2 tide and its M_4 and M_6 harmonics are influenced by wind waves in a different way because of the different contributions from advection and bottom friction. The results of Experiment 3 are qualitatively in agreement with those obtained for the vertical structure of the M_2 tidal flow in the eastern Irish Sea (Davies and Lawrence, 1994a) and for the horizontal structure of the M_2 tidal flow in Cádiz Bay (Kagan et al., 2001).

We now discuss the results of Experiment 4 and emphasise in particular: (i) wind wave/tide interaction and suspended sediment stratification tend to cancel one another out. Hence, depending on which of the two factors prevails (which is determined by the sediment grain size- or u_{*c} and w_s- and wave parameters), the
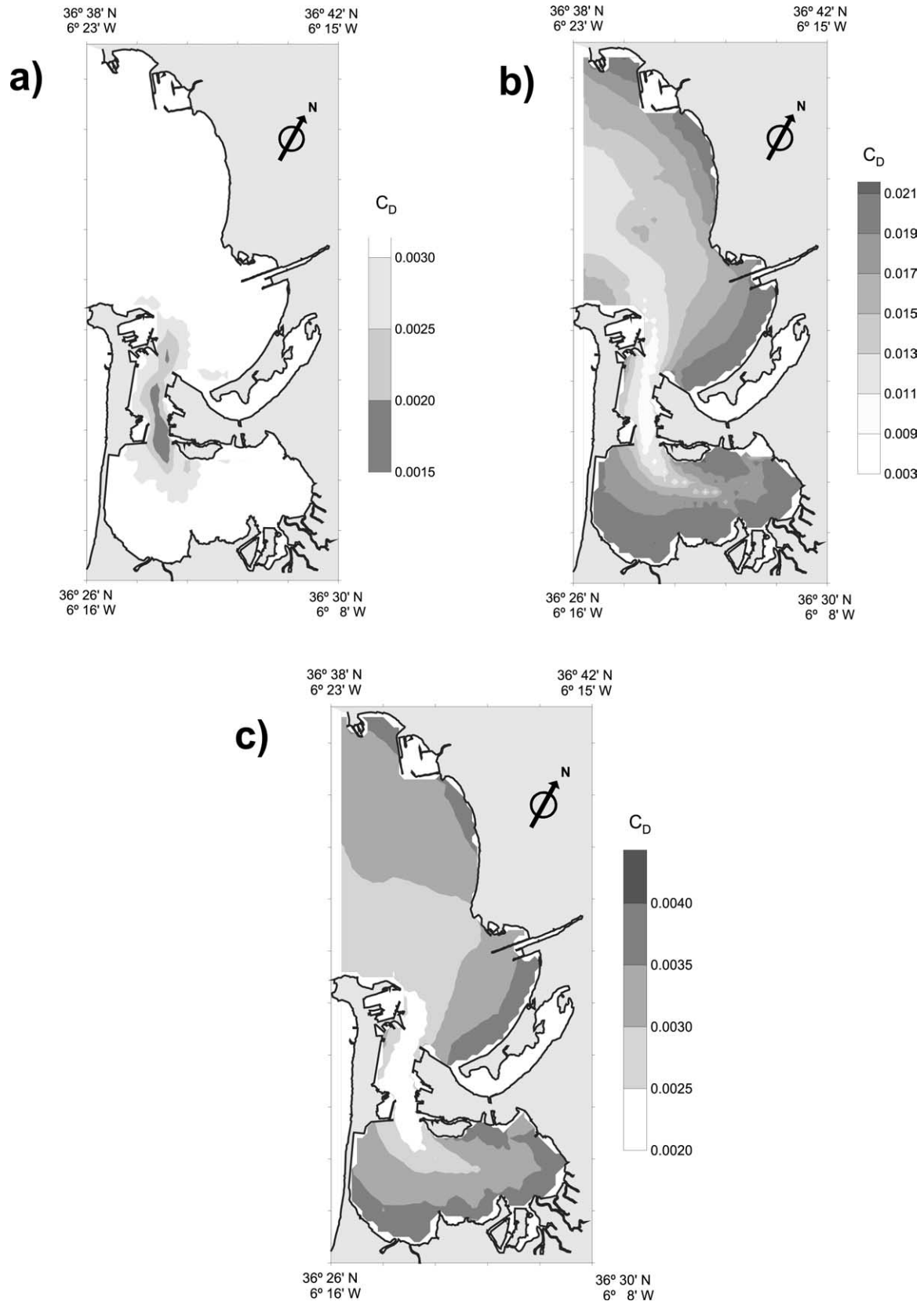
Fig. 2. Drag coefficient predicted with allowance for (a) suspended sediment stratification, (b) wind-wave/tide interaction, and (c) and their combined effect.
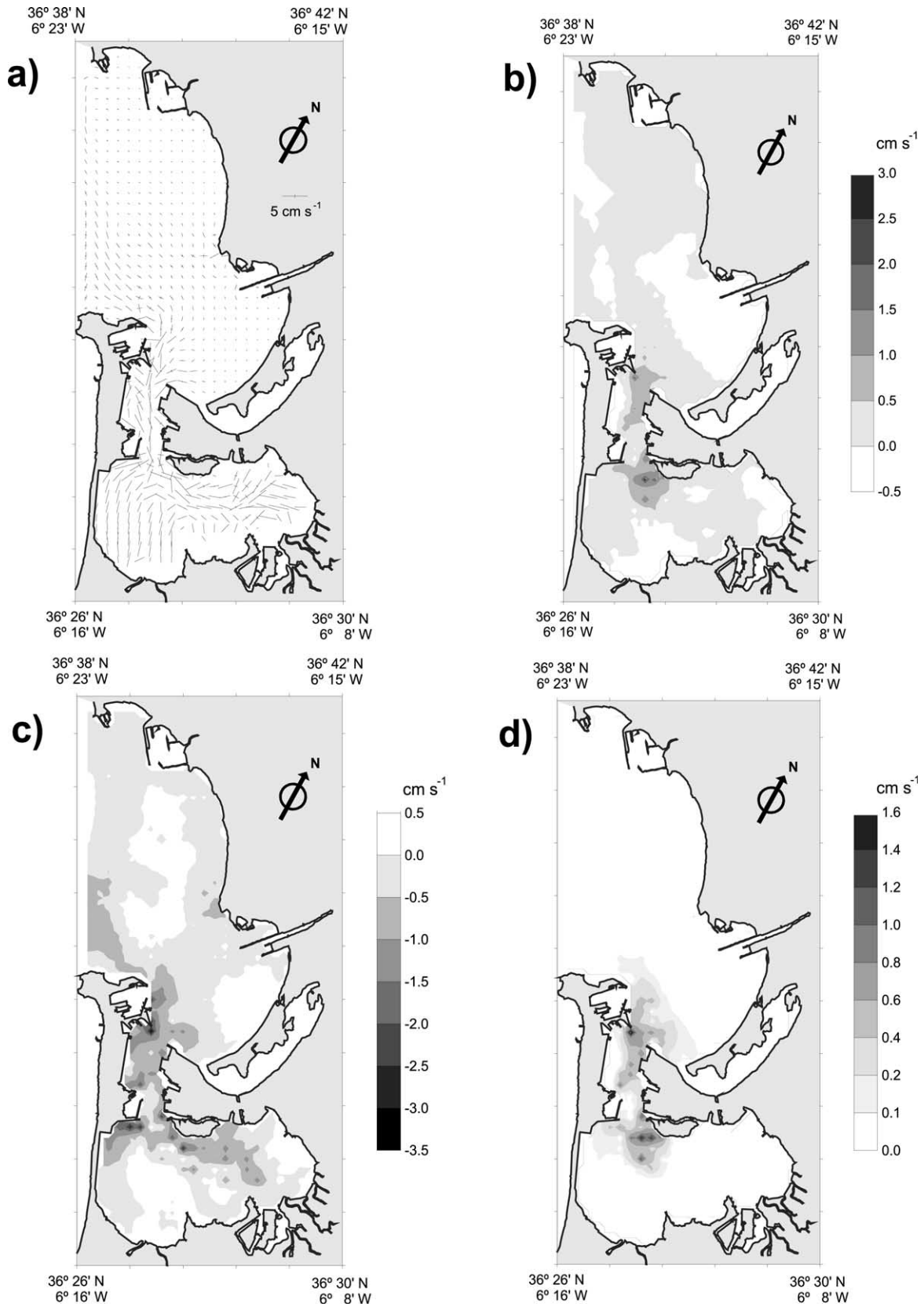
Fig. 3. (a) Predicted major and minor axes of the M_4 tidal ellipses and the changes in maximum depth-averaged tidal velocity due to (b) suspended sediment stratification, (c) wind-wave/tide interaction and (d) their combined effect.
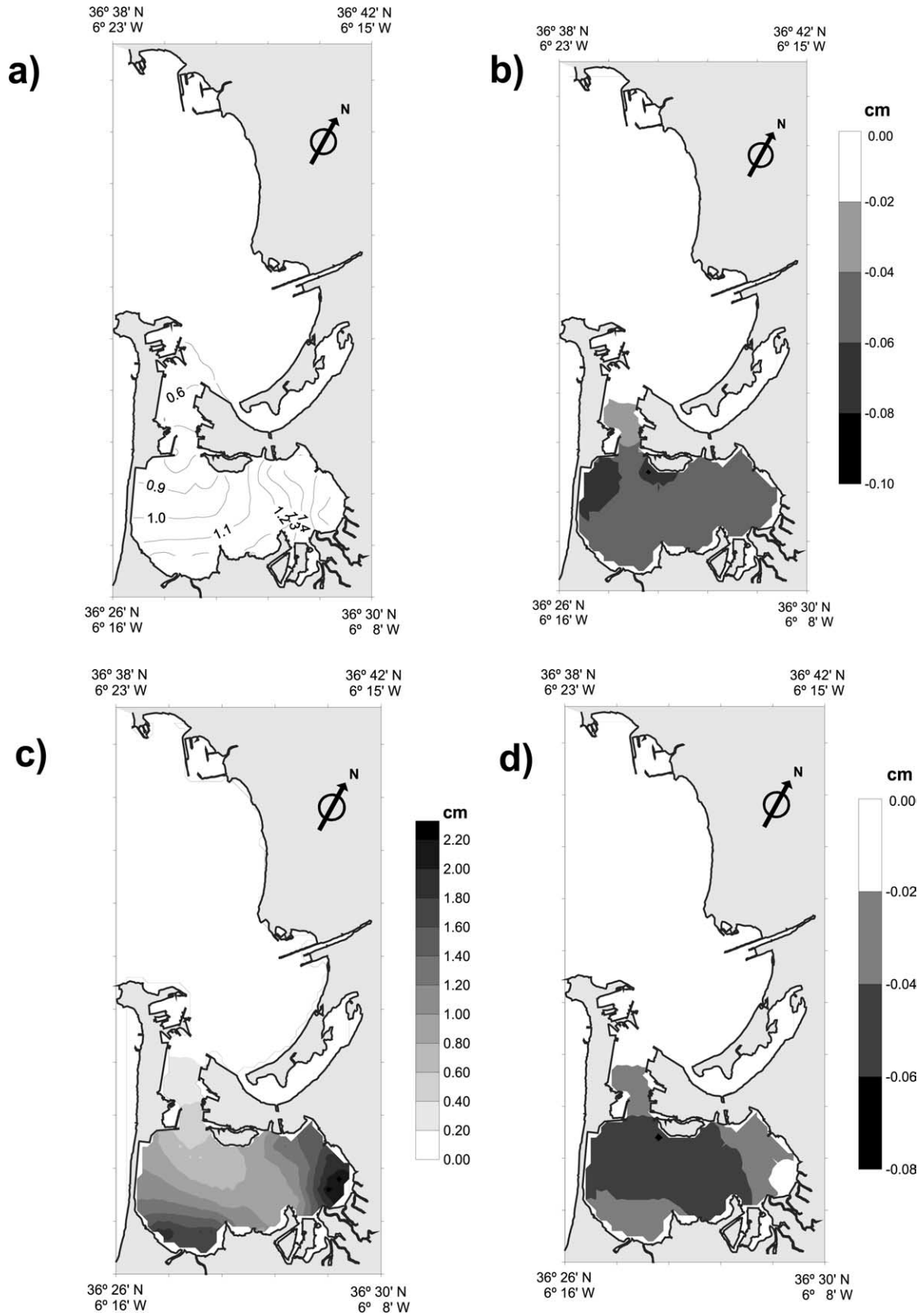
Fig. 4. Predicted amplitudes, in centimetres, of (a) the M_4 tidal elevation and the changes in amplitude due to (b) suspended sediment stratification, (c) wind-wave/tide interaction, and (d) their combined effect.
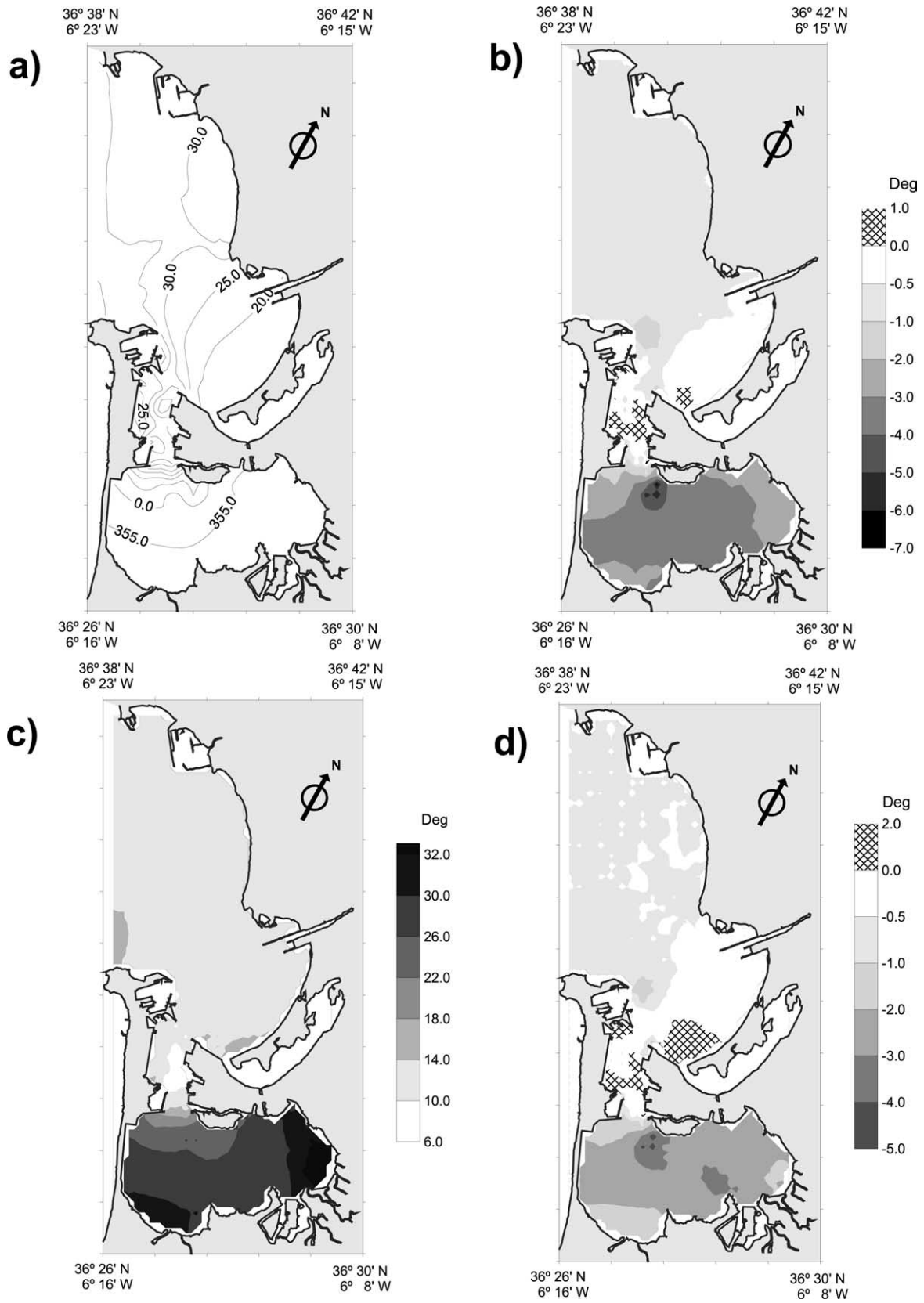
Fig. 5. Predicted phases, in degrees, of (a) the M_4 tidal elevation and the changes in phase due to (b) suspended sediment stratification, (c) wind-wave/tide interaction, and (d) their combined effect.

changes in c_D relative to c_{D0} can be of either sign; (ii) the drag coefficient is a non-linear function of the external parameters determining the vertical structure of the wave and tidal BBLs, so that the dominant influence of a specific factor, corresponding to the limiting cases of no-wave and clear-water flow, varies interactively; (iii) this interaction is difficult, if not impossible, to predict in the general case using elementary physical reasoning or the findings obtained in the limiting cases. The simulation results presented in Figs. 2c and 3d–5d provide support for these considerations; (iv) the model predictions in the general case, especially using the observed tidal elevations and velocities at the open boundary, are in better agreement with observational evidence than those of the specific cases under study (see Table 1).

From Fig. 2c it is apparent that a region with values of c_D less than c_{D0}, where the dominant factor is suspended sediment stratification, occurs only in the Puntales Channel. The remainder of the bay, based on the values of c_D, is within the zone of the dominant influence of wind-wave/tide interaction. This pattern produces an increase in maximum depth-averaged tidal velocity in Puntales Channel and a decrease elsewhere. Accordingly, the tidal elevation amplitudes and phases increase everywhere, except in the Puntales Channel. Nevertheless, these changes in tidal elevation amplitude and phase are very small, being within the accuracy of the model predictions. In other words, the effect of these two factors (wave/tide interaction and suspended sediment stratification) may be thought of as being very nearly balanced. This does not mean, of course, that the conventional assumption employed in tidal dynamics of ignoring wind-wave/tide interaction and suspended sediment stratification is valid. Simply, that in Cádiz Bay at least, their resulting effect vanishes.

5. Conclusions

The formulation of weak-wave/low-frequency current interaction has been extended to the case of suspended sediment-stratified flow. The influence of suspended sediment stratification on flow dynamics is described in terms of a sediment stratification parameter defined as von Karman's constant times the depth-independent function of the relative friction velocity and the relative settling velocity of suspended particles, which is specified by a solution to the problem on the vertical structure of the suspended sediment-stratified near-bottom logarithmic layer.

The formulation of weak wind-wave/tide interaction in suspended sediment-stratified flow is inserted in a 2D non-linear, finite-difference, high-resolution hydrodynamic model and the modified model has been applied to clarify the roles of wind-wave/tide interaction and suspended sediment stratification—individually and in combination—in the formation of the M_4 and M_6 overtides in Cádiz Bay. These factors compete in the sense of their impact on tidal characteristics. Namely, the former is responsible for an increase in the drag coefficient compared to its reference value in the no-wave case and, as a consequence, for a decrease in maximum depth-averaged tidal velocity and an increase in tidal elevation amplitude and phase. The latter factor produces the opposite changes in these characteristics. It has also been shown that due to the dissimilarity of the M_2 tide and the M_4 and M_6 overtides, the conclusions as to the role of the above factors in the formation of the M_2 tide and its M_4 and M_6 harmonics can be quite different. As an example, for the M_2 tide the wave-induced changes in tidal elevation amplitude and phase are of only minor importance, while they are crucial importance for the M_4 and M_6 overtides.

The effects of both the factors taken together have been shown to be very nearly balanced. A comparison of the tidal constants at some sites within the bay, predicted in the wave-affected, suspended sediment-stratified tidal flow and the clear-water tidal flow with no waves, offers an indirect argument in favour of this finding. This does not mean that the conventional assumption of ignoring suspended sediment stratification and wind-wave/tide interaction is valid in shallow-water tidal dynamics, rather that in Cádiz Bay their resulting effects vanishes.

As with other hydrodynamic models, our model is not free of shortcomings. We point out three factors that not only make an accurate prediction of the M_4 and M_6 tidal characteristics difficult but also force us to qualify the present work as at most a case study. These shortcomings are as follows: firstly, in the adopted formulation of weak wind-wave/low-frequency current interaction the real random wave field is represented by a single wave. In addition, parameters of this wave are taken to be invariant throughout the bay except for its very shallow near-coastal regions where the wave amplitude is specified by an empirical wave-breaking criterion. This assumption is reasonable for Cádiz Bay where, because of the absence of significant variations in depth, the waves propagate from the open boundary to the surf-zone without appreciable reflection and backscattering (Kagan et al., 2001). It is hardly valid, however, in other shallow basins.

Secondly, the model for the vertical structure of the suspended sediment-stratified near-bottom logarithmic layer, which provides the basis for the determination of the sediment stratification parameter, uses a one-phase notion of suspension composition to characterise sea-bed sediments, even though observations attest that the sea-bed material in Cádiz Bay consists of two fractions. According to Li and Davies (2001), this assumption tends to be an underestimate of the suspended sediments concentrations at least in the outer part of the suspension

layer in comparison with those predicted using a multiphase notion. This may introduce certain errors into the sediment stratification parameter and then into the drag coefficient and the other sought-for variables.

Thirdly, any one 2D model is incapable in principle of describing the vertical structure of mean velocity. The only option, unless the vertical profile of mean velocity is specified a priori, is to invoke a 3D model complimented by a proper turbulence kinetic energy closure scheme.

A detailed discussion of these aspects of the problem will be presented later.

Acknowledgements

References

Aldridge, J. N., & Davies, A. M. (1993). A high resolution three-dimensional hydrodynamic tidal model of the eastern Irish Sea. *Journal of Physical Oceanography 23*, 207–224.

Álvarez, O., Izquierdo, A., Tejedor, B., Mananes, R., Tejedor, L., & Kagan, B. A. (1999). The influence of sediment load on tidal dynamics, a case study: Cádiz Bay. *Estuarine, Coastal and Shelf Sciences 48*, 439–450.

Álvarez, O., Tejedor, B., & Tejedor, L. (1997). Simulación hidrodinámica en el área de la Bahía de Cádiz. Análisis de las constituyentes principales IV Jornadas Espanolas de Ingeniería de Puertos y Costas. *Servicio de Publicaciones de la Universidad Politécnica de Valencia-98 2125*. 125–136.

Christoffersen, J. B., & Jonsson, I. G. (1985). Bed friction and dissipation in a combined current and wave motion. *Ocean Engineering 12*, 387–423.

Davies, A. M., & Lawrence, J. (1994). Modelling the non-linear interaction of wind and tide: its influence on current profiles. *International Journal of Numerical Methods in Fluids 18*, 163–188.

Davies, A. M., & Lawrence, J. (1994). Examining the influence of wind and wind wave turbulence on tidal currents, using a three-dimensional hydrodynamic model including wave-current interaction. *Journal of Physical Oceanography 24*, 2441–2460.

Davies, A. M., & Lawrence, J. (1995). Modelling the effect of wave-current interaction on the three-dimensional wind driven circulation of the eastern Irish Sea. *Journal of Physical Oceanography 25*, 29–45.

Dean, R. G. (1986). Intercomparison of near-bottom kinematics by several wave theories and field and laboratory data. *Coastal Engineering 9*, 399–437.

Glenn, S. M., & Grant, W. D. (1987). A suspended sediment stratification correction for combined wave and current flows. *Journal of Geophysical Research 92*, 8244–8264.

Grant, W. D., & Madsen, O. S. (1979). Combined wave and current interaction with a rough bottom. *Journal of Geophysical Research 84*, 1797–1808.

Grant, W. D., Williams, A. Y., & Glenn, S. M. (1984). Bottom stress estimates and their prediction on the northern California continental shelf during CODE-1: the importance of wave-current interaction. *Journal of Physical Oceanography 14*, 506–527.

Gutiérrez, J. M., Achab, M., & Parrado, J. M. (1996). Distribution of recent facies at the bottom of the Bay of Cádiz. *Geogaceta 21*, 155–157.

Heathershaw, A. D. (1981). Comparison of measured and predicted sediment transport rates in tidal currents. *Marine Geology 42*, 75–104.

Jonsson, I. G. (1980). A new approach to oscillatory rough turbulent boundary layers. *Ocean Engineering 46*, 75–123.

Kagan, B. A., Schrimpf, W., & Utkin, K. B. (1999). A 'variable' von Kármán's constant as a parameter of suspended sediment stratification. *Izvestiya, Atmospheric and Oceanic Physics 39*, 818–825.

Kagan, B. A., Tejedor, L., Álvarez, O., Izquierdo, A., Tejedor, B., & Mananes, R. (2001). Weak wave-tide interaction formulation and its application to Cádiz Bay. *Continental Shelf Research 21*, 697–725.

Kagan, B. A., & Utkin, K. B. (2000). Weak wave-tide interaction and the drag coefficient in a tidal flow. *Izvestiya, Atmospheric and Oceanic Physics 36*, 566–574.

Li, Z., & Davies, A. G. (2001). Turbulence closure modelling of sediment transport beneath large waves. *Continental Shelf Research 21*, 243–262.

Signell, R. P., Beardsley, R. C., Graber, H. C., & Capotondi, A. (1990). Effect of wave–current interaction on wind-driven circulation in narrow, shallow embayments. *Journal of Geophysical Research 95*, 9671–9678.

Smith, J. D., & Mclean, S. R. (1977). Spatially averaged flow over a wavy surface. *Journal of Geophysical Research 82*, 1725–1746.

Soulsby, R. L., & Wainwright, B. L. S. A. (1987). A criterion for the effect of suspended sediment on near-bottom velocity profiles. *Journal of Hydraulic Research 25*, 341–355.

Tang, Y. M., & Grimshaw, R. (1996). The effect of wind-wave enhancement of bottom stress on the circulation induced by tropical cyclones on continental shelves. *Journal of Geophysical Research 101*, 22705–22714.